ROTORCRAFT PITOT-STATIC SYSTEMS CALIBRATION PROCESS TO REDUCE ERROR IN ALL FLIGHT REGIMES AND ALL ROTORCRAFT CONFIGURATIONS.

***Domenico Vinci**, Lead Flight Test Engineer, domenico.vinci@koptergroup.com, Kopter Group (Switzerland)*
***Luca Casciola**, Flight Test Analysis Engineer, luca.casciola@koptergroup.com, Kopter Group (Switzerland)*

ABSTRACT

Calibration of pitot-static systems is a priority activity to be conducted at the earliest stage of the rotorcraft certification process in order to provide accurate airspeed and altitude flight test data and to develop production pitot-static air data systems with acceptable errors. Legacy air data system did not allow any correction for position error causing great effort for the system design. State of the art Air Data Units allow correction of the airspeed and altitude errors but only for one flight regime and one configuration. Those corrections might present residual errors that are not acceptable for all the other flight regimes and rotorcraft configurations requiring re-design and re-testing.

The paper explains the pitot-static systems calibration method used to discern static and total pressure errors in level flight by field test with the use of a Weather Station. Then it describes the results obtained using the GPS quasi-static Head and Tail wind method. This allowed to obtain calibration data for all flight conditions and for all helicopter configurations using a limited number of flights and without changing the helicopter configuration. The paper explains the equivalence of the level flight results between the NTPS GPS method and the GPS quasi-static Head and Tail wind method and suggests a correction for the Orbis GPS quasi-static technique. A mathematical method is shown to infer calibration curves for pitot systems which guarantee an optimal performance in all the flight conditions and configurations, leading to the creation of lookup tables for the state of art Air Data Units.

Finally, the paper shows a new methodology developed based on a multi-input regressor using a fully connected Neural Network which is capable of providing a correct value of airspeed and pressure altitude in real-time for every aircraft configuration and every flight regime. In this way, the aircraft manufacturer will be able to optimize development and production costs, while having a fully calibrated airspeed in flight. The study provides detail on how to collect flight test data points, pre-processing techniques and analysis. Moreover, the paper describes the findings in optimizing the algorithm structure and in implementing such algorithm in an embedded system.

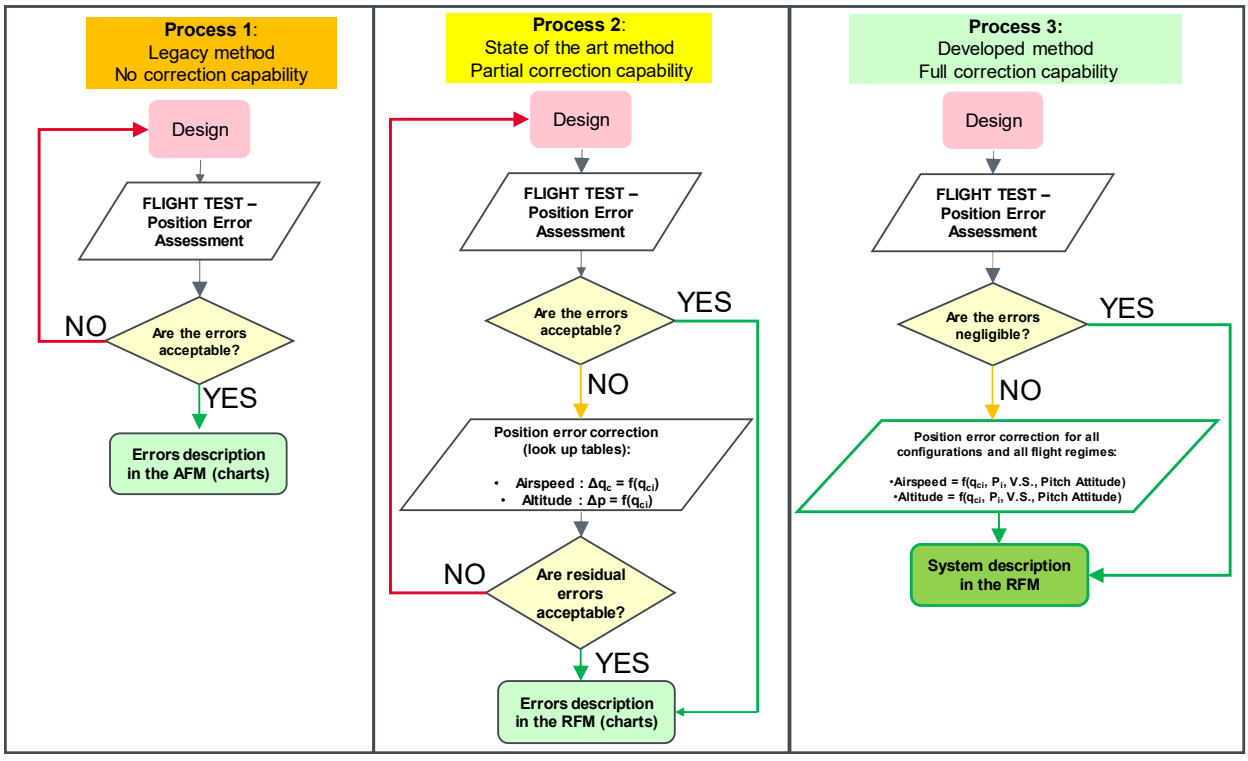

Figure 1 – Pitot static systems calibration processes

1. INTRODUCTION

The FAA and EASA Airworthiness Regulations define the pitot-static requirements and maximum permissible errors for various flight regimes and recommend studying the effects of Gross Weight (GW) and Center of Gravity (CG). Different rotorcraft configurations (mainly longitudinal CG position) and flight regimes (i.e. level flight, climb, descent or autorotation) induce variations of the Angle of Attack (AOA) and Angle of Side-slip (AOS) and consequently changes of in the fuselage aerodynamic field causing a position error (probe's position-dependent error) in the pitot-static systems.

The optimization of the definitive pitot static sensors position and shape (thereafter called production pitot-static as installed in the production aircraft) affects the design of the airframe and the installation of other surrounding components. Although CFD simulations provide insights into the best average probe position, real-world scenarios require in-flight calibration.

Most of the flight test programs use in the early development stages a "temporary" pitot-static sensor installed on a long nose-boom (thereafter called Nose-boom or NB) which ensures pressure measurement not affected by a position error. Classic methods for calibration (i.e. NTPS 3-4 level flight legs GPS method, fly by tower etc…) allow the calibration of production pitot-static systems and the calibration/check of the nose-boom pitot-static system only in level flight condition. More complex and costly methods, such as the use of trailing bomb or a pacer aircraft, are usually employed for calibration in the other than level flight regimes (i.e. climb, powered descent and autorotation). These techniques introduce costs, operational complexity and safety issues (i.e. clearance of the trailing bomb from tail rotor in autorotation).

Legacy air data system did not allow any correction for position error causing great effort for the system design (see Process 1 – Figure 1). State of the art Air Data Units, currently installed on modern rotorcraft, allow the correction of the airspeed (dynamic pressure, $q = P_T - P_s$) and altitude (static pressure P_s) errors to be calculated as a function (lookup table) of only the sensed dynamic pressure (q_{ci}). For every sensed dynamic pressure it is possible to apply corrections Δq_{ci} and $\Delta P_{S,i}$ which usually are fully valid only for one flight regime (usually level flight) and one configuration (i.e. mid CG position). Those corrections might present residual errors that are not acceptable for the other flight regimes and rotorcraft configurations (see Process 2 – Figure 1).

The paper explains the methodology to calibrate the pitot-static systems for forward flight regimes using a limited number of dedicated flight tests, with a direct reduction of time and costs, also ensuring a limited variation in environmental conditions and improved safety.

Taking inspiration from the techniques described in the paper *GPS-BASED Airspeed Calibration for Rotorcraft: Generalized Application for All Flight Regimes, 2020, Denis Hamel & Alex Kolarich*[1] this paper further develops the idea and describes flight testing methods, data analysis techniques and best practices to:

- Obtain calibration data of the pitot static systems for various flight regimes using a limited number of flight tests, with a direct reduction of time and costs, also ensuring a limited variation in environmental conditions and improved safety.
- Calculate dynamic and static pressure corrections for standard Air Data System to minimize the residual error for all the flight regimes and rotorcraft configuration (see Process 2 ***–Figure 1***);
- Define more precise calibration curves for the Air Data Sensors, which go beyond the linear approximation, that allows to obtain calibrated airspeed and altitude for every forward flight condition and CG configuration (see Process 3 – ***Figure 1***). This will ensure a robust Air Data Sensors calibration which does not depend on sensor position and sensor design. In this way, the aircraft manufacturer will be able to optimize production costs, overall aerodynamics and structural integrity while the correction will be managed software side. Pitot-static sensors might be moved closer to the fuselage to increase safety for ground operations. Moreover, in the case of new modifications that could affect the calibration of the installed pitot-static systems, the techniques will allow to generate a new calibration by flying a reduced number of flights, and without requiring hardware changes in the pitot-static system.

2. GPS-BASED CALIBRATION

2.1 General derivation of calibration

The calibration of air pressure probes involves the execution of dedicated flight testing activity. The datum measured by the un-calibrated probes is compared against a reference calibrated datum (provided by a calibrated sensor or calculated). The difference between the two constitutes the error of the un-calibrated probes. By collecting this information in the form of interpolating function or look-up tables including the dependency on other monitored parameters, it is possible to calibrate the probes.

It is very convenient to use GPS and inertial measurement unit (IMU) data corrected for the density ratio to obtain the reference speed for the aircraft. However, the GPS and IMU recordings include and do not separate the effect of the wind from the actual dynamic pressure (see **Figure 2**).

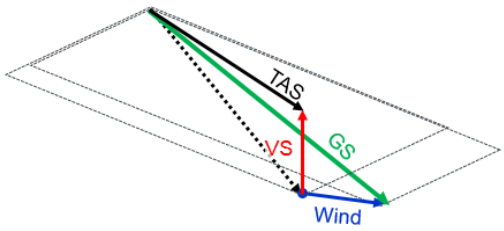

Figure 2- Wind effect on the measure of TAS

The presence of the wind during the execution of calibration flights could introduce significant errors and the direct comparison of an airspeed datum with a GPS+IMU (corrected for density) datum would not be possible without the use of several mathematical techniques: In the study those techniques were applied and the result compared.

For the sake of clarifying the concepts de following definitions are used:

- $\boldsymbol{IAS}$: Indicated Airspeed as displayed by the instrument of the aircraft. IAS is affected by the position error, function of flight regime and configuration.
- $\boldsymbol{IAS_{corr}}$: Air speed indicated corrected by a correction function. Ideally, the IAS correction function should cause $IAS_{corr} = CAS$. State of the art systems accept a single calibration function that is only valid for one flight regime and aircraft configuration (typically level flight and longitudinal mid-CG). Therefore, non-negligible residual errors could affect IAS_{corr} when combining different flight regimes and aircraft configurations (thus in general $IAS_{corr} \neq CAS$).
- $\boldsymbol{CAS}$: Calibrated Airspeed, the real measure of the dynamic pressure generated on the rotorcraft, excluding the effect of compressibility.
- $\boldsymbol{EAS}$: Equivalent airspeed, calibrated airspeed adjusted for compressibility effects. For rotorcraft usually operating at low Mach number and not at 'high altitude' (less than 20,000 feet), $EAS \cong CAS$ (negligible compressibility effect) is assumed.
- $\boldsymbol{TAS}$: True airspeed is the actual speed of the aircraft through the air surrounding it.
- $\boldsymbol{WIND}$: The velocity of the wind with respect to the ground local vertical coordinate system. Often it is supposed that the wind is always parallel to the ground. The wind component is usually unknown and non-negligible.
- $\boldsymbol{VS}$: The Vertical Speed represents the vertical component of CG rotorcraft speed.
- $\boldsymbol{GS}$: Ground Speed, the speed of the aircraft CG with respect to the ground local vertical coordinate system.

Starting from the GS, removing the effect of the $Wind$ vector and adding the vertical component (VS vectors) the result is TAS (see **Figure 2**).

Once the TAS is calculated, it is possible to apply the density correction and obtain the CAS.

Regarding the altitude, the following conventions are used:

- The prefix $\boldsymbol{WS}$ indicates that the datum comes from the Weather Station.
- The prefix $\boldsymbol{HC}$ indicates that the Rotorcraft/Helicopter datum.
- The subscript $\boldsymbol{tape}$ indicates the GPS altitude from Standard Sea Level (SSL).
- The subscript $\boldsymbol{calib}$ indicates the actually calibrated variables.
- The subscript $\boldsymbol{ref}$ indicates that the value estimated according to ISA equations.

2.2.1 Field method

Most GPS pitot-static calibration methods allow the calculation of airspeed calibration curves by measuring the combined effect of static and total pressure errors. Unless one assumes the hypothesis that 'all error is in the static port' (total pressure error-free), there is no possibility of separating the two errors. While the assumption is usually valid for fixed-wing applications, in the case of rotary-wing aircraft, this is not always the case, as rotors wash can add energy to the Total Pressure port.

The following 'field method' (see **Figure 3**) was developed to accurately measure the error in the Static Pressure port for a configuration and one level flight airspeed, at Mollis Airport (direction runway, RWY 01/19) and using data from the Weather Station (WS - Vantage PRO2):

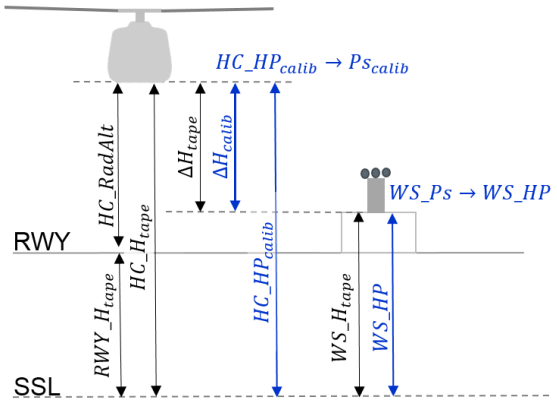

Figure 3- Field method

The WS provided data are: Ambient P_s (WS_Ps , with altitude set to $0ft$), Outside Air Temperature (WS_OAT converted to [K]) and Relative Humidity (WS_RH).

From the HC latitude, it is possible to obtain the Runway tape height instantaneously overflown by the HC (note Mollis RWY has a constant slope):

$$RWY\_H_{tape} = 112748 - 2363.72 * HC\_GPS\_lat[deg] \quad (1)$$
$$for: 47.071077 < HC\_GPS\_latitude < 47.084615$$

The HC tape altitude (4ft is the static port height above the zero RadAlt level) and delta tape are obtained:

$$HC\_H_{tape} = RWY\_H_{tape} + HC\_RadAlt + 4\,[ft] \quad (2)$$
$$\Delta H_{tape} = HC\_H_{tape} - \underbrace{WS\_H_{tape}}_{1512\,[ft]} \text{ (WS at 1512 ft)} \quad (3)$$

Calculate the WS pressure altitude:

$$WS\_HP = \frac{T_{SSL}}{a_{SLL}}\left[1 - \left(\frac{WS\_Ps_{ambient}}{P_{SSL}}\right)^{\frac{a_{SLL}R'}{g}}\right] \quad (4)$$

Where constants and Standard Seal Level (SSL) parameters are:

$$R' = g_c R = 32.17 * 96.034; \quad \gamma = 1.4; \quad g = 32.174049$$
$$a_{SLL} = 0.001982\ K/ft\ ; \quad a = 661.48\ [kt]$$
$$P_{SSL} = 1013.25\ [hPa];\ T_{SSL} = 288.15\ [K];$$
$$\rho_{SSL} = 1.225\ [kg/m^3]$$

Obtain the calibrated altitude difference and Ps_{calib} (referred to HC) from the ΔH_{tape}.

$$\Delta H_{calib} = \Delta H_{tape} \frac{T_{SSL} - a_{SLL} * WS\_HP}{WS\_OAT} \quad (5)$$

Note: WS OAT is used as best reference.

$$HC\_HP_{calib} = WS\_HP + \Delta H_{calib} \quad (6)$$

$$Ps_{calib} = P_{SSL} \left[1 - \frac{a_{SLL} * HC\_HP_{calib}}{T_{SSL}}\right]^{\frac{g}{a_{SLL}R'}} \quad (7)$$

Compute the static pressure and altitude pressure errors of the generic system X:

$$X\_Ps_{error} = Ps_{calib} - X\_Ps \quad (8)$$

$$X\_HP_{error} = HC\_HP_{calib} - X\_HP \quad (9)$$

The next steps allow the errors in the dynamic pressure and Pt to be calculated. Note that the influence of humidity is to reduce the density by usually a small amount (around 2% density reduction from the dry is recorded at 38°C). The following steps describe the calculation of dry and wet air density ratio (σ_{dry} *and* σ_{wet}).

Compute pressure of vapor saturation:

$$Psat_{vapor}[psF] = 2.685 + 0.003537 * WS\_OAT\ [F]^{2.245} \quad (10)$$

$$Psat_{vapor}[hPa] = [psF] * 0.4788 \quad (11)$$

Compute the density ratio in dry conditions from equation of state:

$$\sigma_{dry} = \frac{Ps_{calib}}{P_{SSL}} \frac{T_{SSL}}{WS\_OAT} \quad (12)$$

Calculate the sigma wet by applying the correction for the RH.

$$\sigma_{wet} = \sigma_{dry} \left[1 - \frac{0.378 * WS\_RH * Psat_{vapor}}{Ps_{calib}}\right] \quad (13)$$

Use the ground speed to calculate the CAS. In case of wind two opposite courses are flown to remove the wind component.

$$CAS = GS[kts]\sqrt{\sigma_{wet}} \quad (14)$$

Compute the total pressure error:

$$Pt_{calib} = Ps_{calib} + P_{SSL} \left\{\left[\frac{\gamma-1}{2}\left(\frac{CAS}{a}\right)^2 + 1\right]^{\frac{\gamma}{\gamma-1}} - 1\right\} \quad (15)$$

$$X\_Pt_{error} = Pt_{calib} - X\_Pt \quad (16)$$

Compute the airspeed error of system X:

$$X\_CAS_{error} = CAS - X\_IAS \quad (17)$$

Figure 4 show the result of the calculation of the Ps and Pt errors of the ESIS production system in level flight. Two opposite courses (Head Wind – HW and Tail Wind - TW) were conducted at each airspeed. The plot shows (solid lines) the increased with dynamic pressure of the Ps error while the Pt error was negligible.

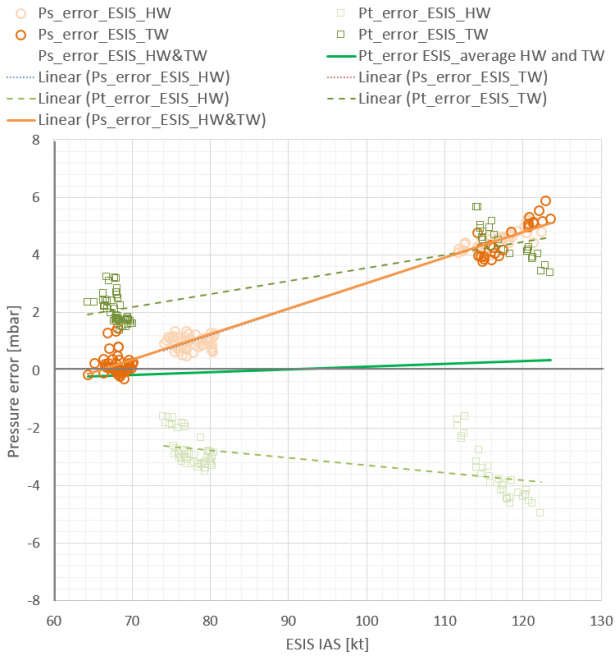

Figure 4- Field Method – Calculation Ps and Pt errors for production pitot static system

2.2.2 GPS static vs quasi static method results

The research started by using the NTPS airspeed calibration method described in the paper *Using GPS to accurately establish True Airspeed (TAS), 1998, Doug Gray*[1]. The method consists of flying at least three legs in offset directions at equal IAS (constant during the test point) keeping a steady heading. If the three legs are flown in an area where the wind is constant in magnitude and direction, by constructing a triangle of velocities it is possible to know the wind magnitude and direction and therefore to calculate CAS. The method is widely used by rotorcraft manufacturers, but has several limitations that make it incomplete, very expensive and time-consuming:

- The method is only valid for level flight.
- Calibration data is only valid for the flown configuration. To record calibration data for the forward and rear CG, the configuration must be changed;
- Several stable test points are performed at discrete airspeeds in the calibration range;

The *GPS-based Airspeed Calibration for Rotorcraft (Generalized Application for All Flight Regimes) method*[2] was then employed. The method allows to repeat the position errors measurement in level flight and extend to various flight regimes (climb, descent and autorotation) and longitudinal CG configurations. The method, hereafter referred as HW-TW GPS quasi-static method, suggests to reduce the legs to two, flying in the head and tail wind directions for the removal of the wind component. TAS is calculated as result of the vertical component (VS) and horizontal component (see **Figure 5**). Horizontal component of the TAS is obtained from the GS removing the wind component. Our experience has demonstrated

that, in case of unknown wind condition, it is possible in short time to determine in flight (just comparing GS and IAS in two or three short legs) the direction of the wind with enough precision.

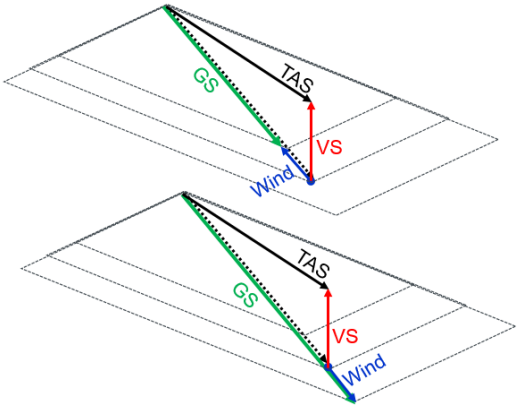

Figure 5- HW (above) and TW (below) method calculation (reference system integral with the air mass).

In addition, the paper suggests to perform the test by flying only in one configuration (i.e. longitudinal mid CG) and "quasi-statically" covering the entire airspeed range by flying at a constant deceleration speed to simulate the effect of a rear CG configuration and with a constant acceleration to simulate the effects of forward CG.

We demonstrated on the AW09 Prototype 3, that accelerations and decelerations of 1kt/s could induce a Pitch vs Airspeed characteristic comparable to, or slightly higher than (thus conservative for the scope), the ones introduced by a shift of the longitudinal CG position between the foremost and astern location (see **Figure 6**).

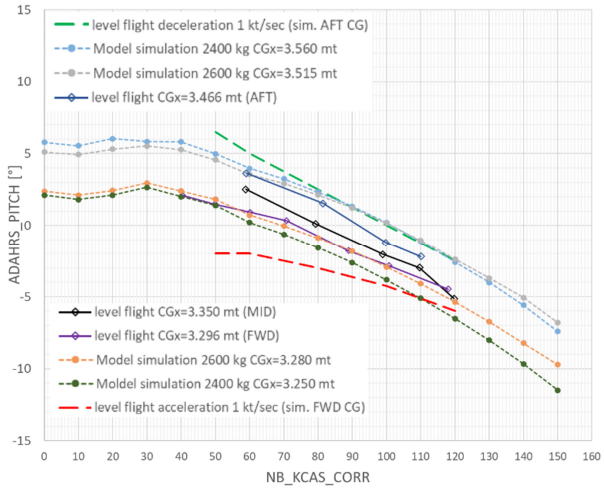

Figure 6- Pitch Attitude

This indicates that, for the case in consideration, repeating the same HW-TW method both in acceleration and deceleration of 1kt/s or slightly higher, it is possible to obtain the calibration data also for full forward and full aft CG configurations (extreme of the envelope). In general, having prior knowledge of the attitude of the helicopter in the various flight regimes will allow manufacturers to identify the best acceleration/deceleration rate to simulate the full CG position shift.

Comparison of level flight results between the NTPS static GPS (fixed airspeed) and HW-TW quasi-static GPS (acceleration/deceleration) methods shows that they provide the same airspeed calibration curves. Both methods resulted in the nose-boom being affected by a small “under-reading” error, a consequence of the increase of pressure in front of the helicopter nose. Also the resulting error was not really affected by the configuration.

As it is shown in **Figures 7 to 10**, the calibrations obtained using the NTPS method in level flight (black dashed line) coincided with the calibration obtained using the average of the calibration HW (green line) and the calibration in TW (blue line). The two figures depict respectively the calibration for the nose-boom air data system and for the ADAHRS production system. It should be noted that the offset between the HW and TW lines is the effect of the wind.

Ideally, in no-wind or very weak wind conditions, even with sporadic wind disturbances, the green and blue lines (nominally HW and TW) will tend to coincide. In theory in no-wind condition only one leg in whatever direction is enough. Anyway, the results suggested to always perform two opposite HDG courses. In fact, the strength of the quasi-static HW-TW method and the subsequent data reduction lies in the continuous averaging that eliminates the wind perturbation and generates the correct calibration regression for every flight condition.

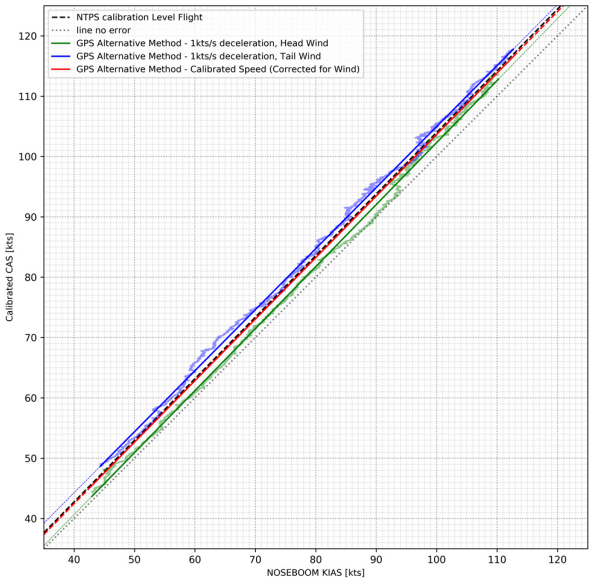

Figure 7– Nose-boom, HW-TW calibration - Deceleration

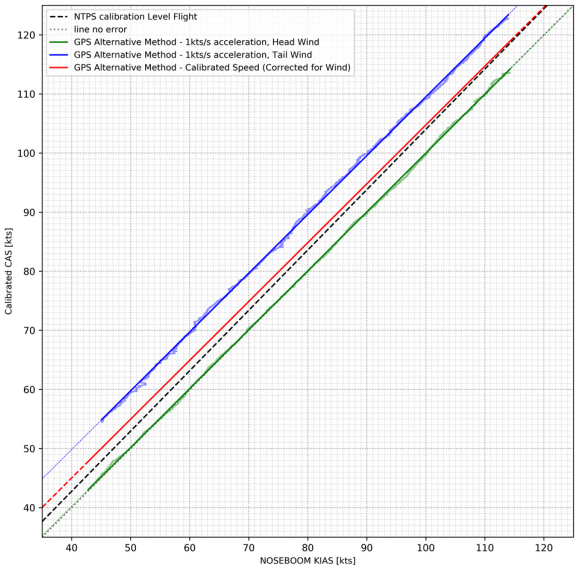

Figure 8– Nose-boom, HW-TW calibration - Acceleration

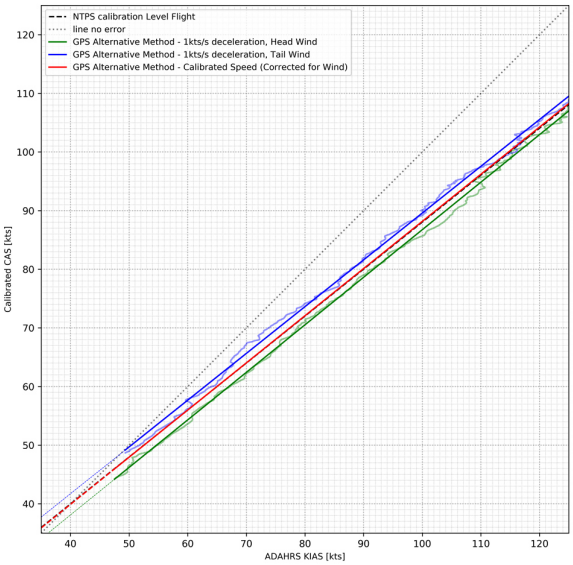

Figure 9– ADAHRS, HW-TW calibration - Deceleration

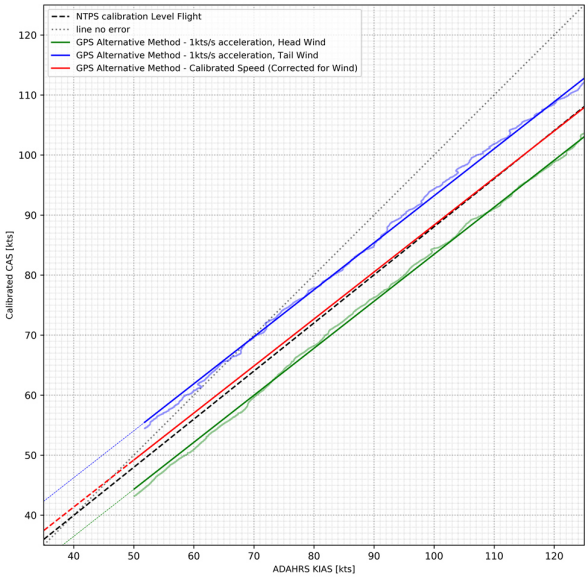

Figure 10– ADAHRS, HW-TW calibration - Acceleration

2.2.3 Correction of ORBIS method

Before proceeding further, the research developed a modification of the original ORBIS method calculation described in the paper [**Ref 2**]. The ORBIS method consists in executing a spiral maneuver using a constant bank angle, while accelerating or decelerating to simulate a shift in CG longitudinal position. By comparing the GS and the indicated helicopter heading $\Psi_{HC|comp}$, it is possible to determine the wind component.

The method at first did not provide matching results with the NTPS method and was disregarded, however by applying a correction to the helicopter heading datum based on the AOA and the AOS, it is possible to significantly improve the convergence and precision of the ORBIS.

The heading is corrected by the presence of helicopter roll φ, Angle of Attack AOA and Angle of Sideslip AOS:

$$\Psi_{HC} = \Psi_{HC|compass} + AOS\ \cos(\varphi) - AOA\ \sin(\varphi) \quad (18)$$

For each point in time it is possible to construct the following equations:

$$GS\cos(\Psi_{Track}) = TAS\cos(\Psi_{HC|comp}) + Wind\cos(\Psi_{Wind}) \quad (19)$$

$$GS\sin(\Psi_{Track}) = TAS\sin(\Psi_{HC|comp}) + Wind\sin(\Psi_{Wind}) \quad (20)$$

Where TAS, $Wind$ and Ψ_{Wind} are three unknowns. It is possible to collect multiple test points over the ORBIS test and create an over-determined system which brings to the derivation of the three unknowns. To solve the system of equations, we used the Moore-Penrose pseudoinverse[3].

Plots in **Figures 11 to 14** show the result of the ORBIS method for the Nose-boom calibration.

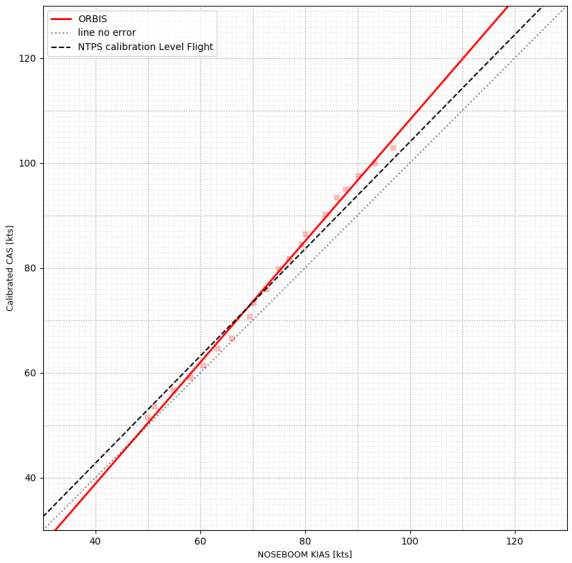

Figure 11 – Nose-boom, Level flight ORBIS calibration, deceleration left hand turn - Classic calculation results

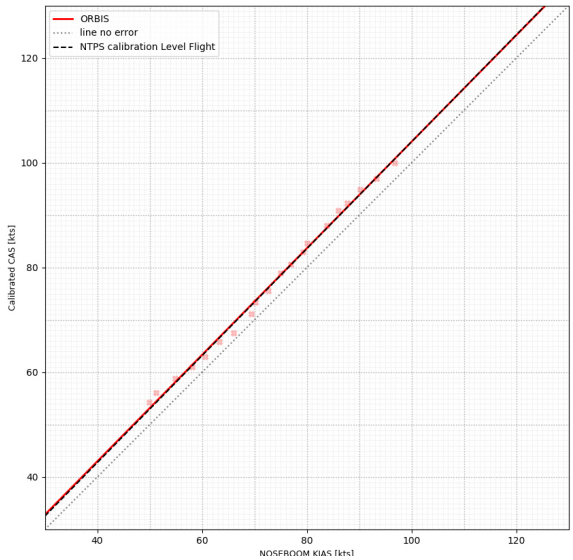

Figure 12 – Nose-boom, Level flight ORBIS calibration, deceleration left hand turn - Proposed calculation results

Despite the ORBIS technique allowing to obtain the calibration flying only 1 leg, compared to the 2 needed in the HW-TW method, it proved to have serious limitations (likely rotorcraft handling qualities dependent) when applied to autorotation and climb and descent, and provided sufficiently accurate data only in level flight. Therefore, the technique was not used further in the calibration tests program.

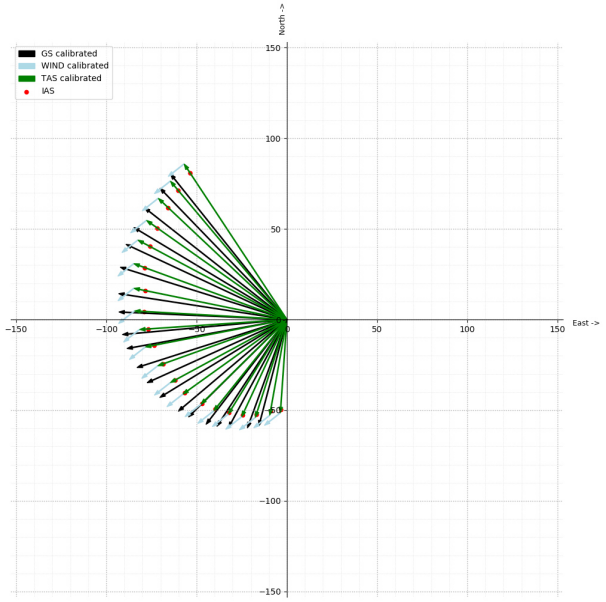

Figure 13 – Nose-boom, Level flight ORBIS vector calculation, Classic method

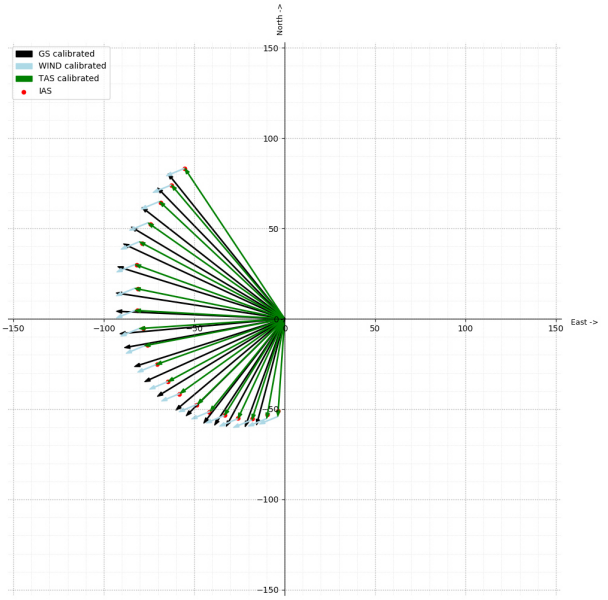

Figure 14 – Nose-boom, Level flight ORBIS vector calculation, Proposed correction

3. GENERALIZED CALIBRATION FOR ALL FLIGHT CONDITIONS AND CG LONGITUDINAL POSITION

3.1 Airspeed calibration for all flight regimes

Comparison of the HW-TW method results between nose-boom and production pitot static systems, indicated that it might be possible to obtain a calibration of the pitot-static systems in all the flight conditions: level flight, climb, powered descent and autorotation. Further tests are planned to compare the HW-TW method results in climb, powered descent and autorotation with an alternative recognized method (i.e. trailing bomb). The test points executed in deceleration were representative of an Aft CG

position, while the test points executed in acceleration were representative of a Forward CG position. We can assume without introducing a significant error that the average line between the Acceleration and Deceleration is representative of a Mid CG position. It is therefore possible to represent all the airspeed errors in a common plot, like in **Figure 15**.

The plot shows the airspeed error recorded by the ADAHRS air data system recorded in all flight conditions. As we can see the probe is mostly over-reading, meaning that the probe is located in a position where the flow field Pressure Coefficient $CP < 0$.

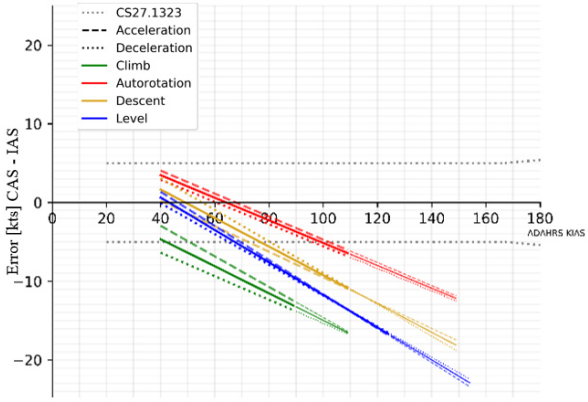

Figure 15 - HW-TW, ADARS errors for all flight regimes (note: solid line representative of mid-CG position)

Defining the look-up table to feed into the Air Data Unit, would correct only one flight condition and configuration, and a residual error would still exist for the other combinations of flight condition and configuration (**Figure 1**, Process 2).

To determine the effect that the chosen correction would have on the various flight regimes, it is possible to compute the residual errors in post-processing, rather than collecting data in flight testing. We denote with (see **Figure 16**):

- $\boldsymbol{\alpha_{corr}}$, $\boldsymbol{\beta_{corr}}$: regression coefficients of $\boldsymbol{IAS_{corr} = f(IAS)}$. This is the correction that can be applied in the state of the art Air Data System.
- $\boldsymbol{a_{IAS}}$, $\boldsymbol{b_{IAS}}$: regression coefficients of regression coefficients of $\boldsymbol{CAS = f(IAS)}$.
- $\boldsymbol{a_{IAS\_corr}}$, $\boldsymbol{b_{IAS\_corr}}$: regression coefficients of $\boldsymbol{CAS = f(IAS_{corr})}$.
- $\boldsymbol{\Phi_{IAS\_corr|Err}}$, $\boldsymbol{\psi_{IAS\_corr|Err}}$: regression coefficients of airspeed residual error after correction $\boldsymbol{CAS - IAS_{corr} = f(IAS_{corr})}$ (see **Figure 17**).

It is possible to calculate the residual error of a given correction using the following equations:

$$\boldsymbol{a_{iasCorr}} = \frac{a_{ias}}{\alpha_{corr}} \quad (21); \quad \boldsymbol{b_{iasCorr}} = b_{ias} - \beta_{corr}\frac{a_{ias}}{\alpha_{corr}} \quad (22)$$

$$\boldsymbol{\Phi_{iasCorr\backslash Err}} = \frac{a_{ias}}{\alpha_{corr}} - 1 \quad (23);$$

$$\boldsymbol{\psi_{iasCorr\backslash Err}} = b_{ias} - \beta_{corr}\frac{a_{ias}}{\alpha_{corr}} \quad (24)$$

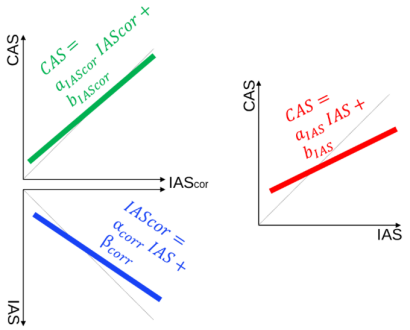

Figure 16– Schematics for derivation of calibration after the correction has been applied

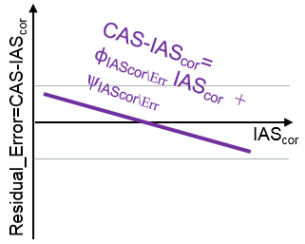

Figure 17– Schematics for derivation of calibration residual error

Knowing the regression coefficients for every line, it was possible to determine the calibration function minimizing the error for a desired condition.

Several correction strategies (optimization of $\boldsymbol{\alpha_{corr}}$, $\boldsymbol{\beta_{corr}}$) were evaluated to reduce the airspeed residual error for the ADAHRS and ESIS production systems: the standard calibration based on level flight curves offered a very low airspeed error in straight and level flight (full CG envelope), but it did not respect the target airspeed error limitations of ±5kts in autorotation and in climb (see plots in **Figure 18**).

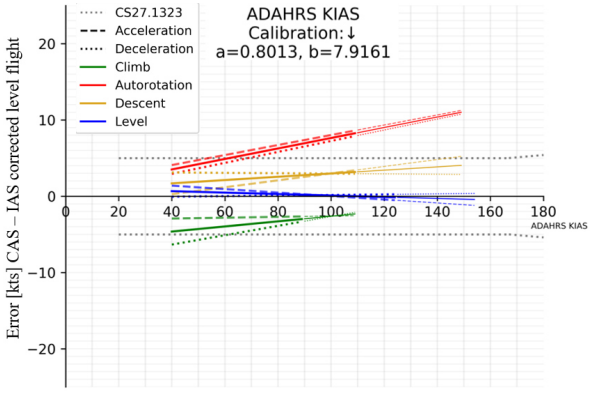

Figure 18 - HW-TW, ADARS residual errors for all flight regimes.

It was possible to define the best correction curve that ensures that the airspeed error is between the ±5kts limits in all the four flight regimes and for every possible CG configuration and that no IAS and Altitude mismatch are generated between the production pitot-static systems. A tailored/blended model correction was developed targeting a balanced error between the two extremes, over-reading (climb with aft CG) and under-reading (autorotation forward CG) up to 120kts IAS, while the calibration keeps the level

flight error constant and over-reading by 3kts above 120kts IAS (see **Figure 19**). This resulted in a constant residual error of 5 Kts under-reading (easy to remember in flight) in the auto rotational airspeed range. In addition, autorotation airspeeds above 120 Kts are considered operationally not a concern as in practice in case of engine failure for a single engine helicopter the airspeed is immediately reduced below power-off never-exceed airspeed ($V_{NE,power-off}$). Also for the high airspeed speed range the level flight indicated airspeed is slightly over-reading (safe-side).

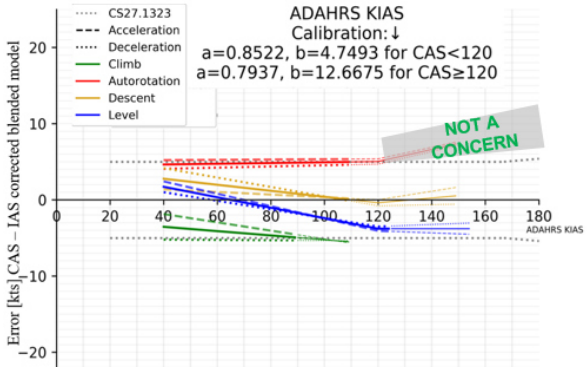

Figure 19- HW- TW, ADAHRS residual errors in the various flight regimes after tailored/blended calibration

3.2 Pressure Altitude calibration for all flight regimes

In addition to the filed method (see para 2.2.1) further investigation confirmed that the Static Pressure (Ps) is the cause of errors. From **Figures 20** and **21** it is possible to see that the Static Pressure Coefficient CP varies quite significantly with AOA and AOS, while the Total Pressure (Pt) remains almost constant for variations of those.

This fact implies that in all the flight conditions and configurations the rotor downwash is not adding energy and altering the Pt sensed by the pitot tubes. Based on this result and following a similar approach to calibrated airspeed calculation (see formulas 15), it has been possible to calculate the Pressure Altitude (HP) error as follow:

$$Ps_{calib} = Pt - P_{SSL}\left\{\left[\frac{\gamma-1}{2}\left(\frac{CAS}{a}\right)^2 + 1\right]^{\frac{\gamma}{\gamma-1}} - 1\right\} \quad (25)$$

$$X\_HP_{error} = \frac{T_{SSL}}{a_{SLL}}\left[1 - \left(\frac{Ps_{calib}}{P_{SSL}}\right)^{\frac{aR'}{g}}\right] - X\_HP \quad (26)$$

Figure 22 shows the calculated HP error of the ADAHRS production pitot-static system without correction. Similarly, to the correction for airspeed, several correction strategies were evaluated to reduce the altitude error for the ADAHRS and ESIS.

As can be seen in **Figure 23**, the blended correction (used for airspeed) provided better results in autorotation at high speeds (range of no operational importance) at the expense of less optimal results in level flight and climb. Thus this strategy was discharged.

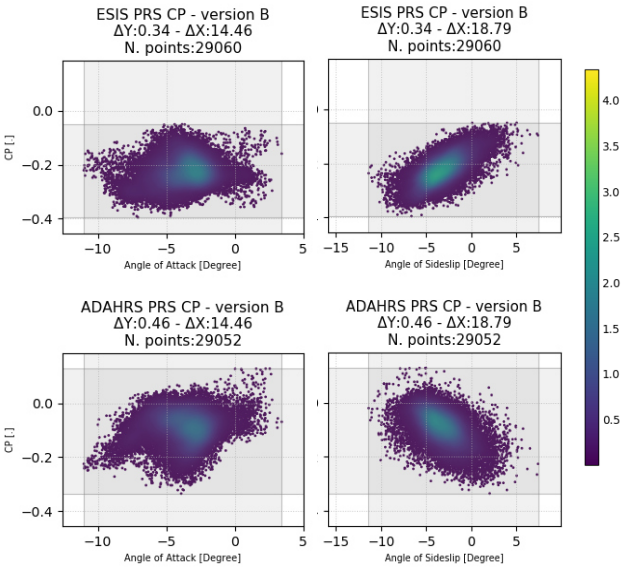

Figure 20 –Scatter plots of CP versus AOA and AOS (color scale according to probability distribution)

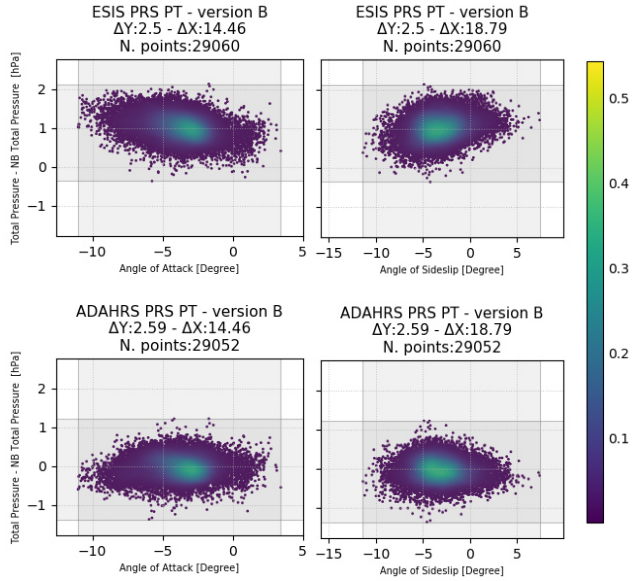

Figure 21 –Scatter plots of P_t (nose-boom sensor as reference) versus AOA and AOS (color scale according to probability distribution)

The correction for level flight (**Figure 24**) was chosen because more emphasis was placed on reducing the error under level flight conditions. Also in autorotation the selected altitude correction strategy provides an altitude under-reading (therefore conservative).

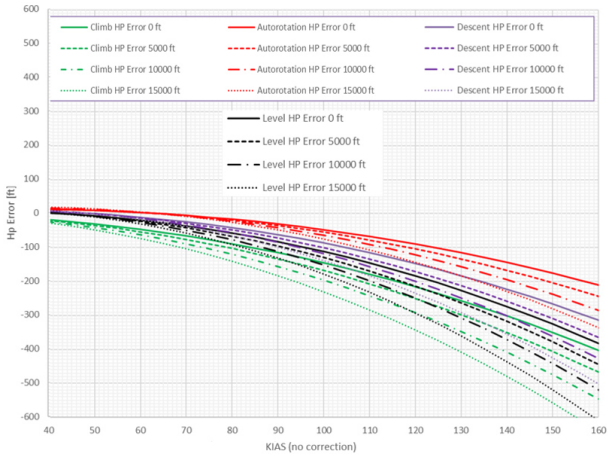

Figure 22 –ADAHRS, HP error, No correction applied

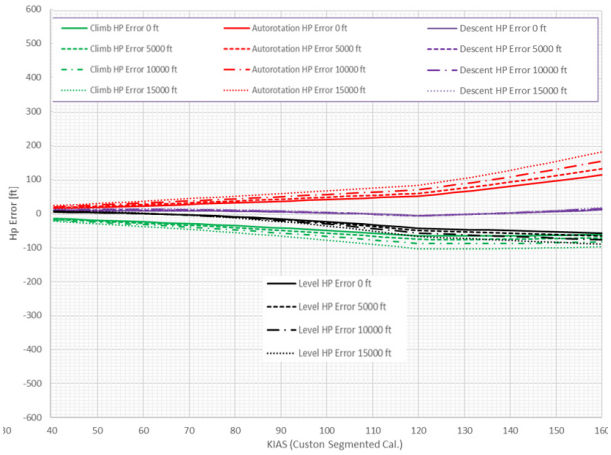

Figure 23 –ADAHRS, HP error, Tailored/blended calibration (as for level flight)

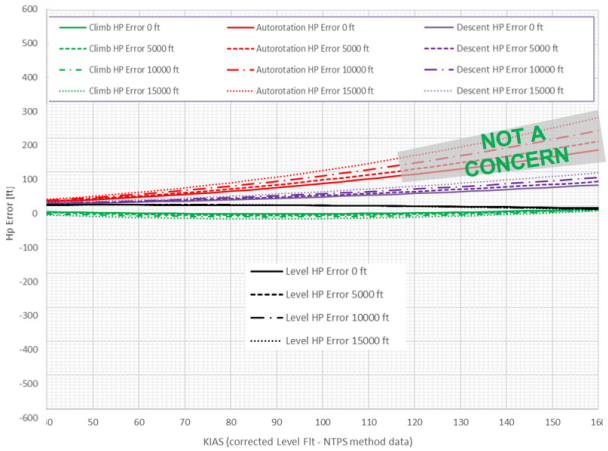

Figure 24 –ADAHRS, HP error, Correction applied for Level Flight

4. DEVELOPMENT OF A GENERAL MULTI-INPUT REGRESSOR FOR REAL-TIME CALIBRATION

4.1 Preface

None of the existing methods and state-of-the-art air data systems are able to correct production pitot-static data (airspeed and altitude) for all configurations and all flight regimes as they use only the dynamic pressure parameter. Consequently, there is always the risk of redesigning and re-testing if residual errors are not acceptable or cause an out-of-bounds difference between productions pitot-static systems.

It should be noted that for the AW09 prototype the pitch attitude slope with respect to airspeed is generally 'flat'. This means that the effects of flight conditions and configurations are potentially limited compared and other rotorcrafts. Furthermore, the need to move the pitot-static sensors (i.e. closer to the fuselage) could lead to results that cannot be corrected.

4.2 Development of calibration algorithm

The last part of the research was aimed at generalizing the calibration procedure to obtain the capability of the air system to correct for positions errors for every flight regimes and rotorcraft configurations with the least flight test effort. Using principal component analysis techniques[4], allowed us to identify the parameters (in addition to the static and dynamic pressure) which directly influence the error of production datum, which are Pitch angle and Vertical Speed. Hence the idea of interpolating the data with a multi-dimensional regression function (see **Figure 25**) using parameters always available in the aircraft production configuration as input.

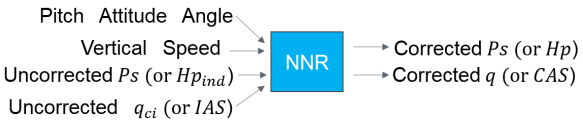

Figure 25–Neural Network Regressor for pitot-static correction

Required training data input and output are obtained by planning a limited flight activity where the helicopter covers the flight envelop with a variety of maneuvers in different configurations. Hereafter a combination of flight conditions and configurations for minimum acquisition data:

1. Maneuvers:
   - level flight,
   - climb (at least two rates equally spaced in the possible envelope: i.e. 500 and 1000 ft/min),
   - powered and not-powered descent (at least three rates equally spaced in the possible envelope up to autorotation/non powered descent: i.e. 700, 1400 and 2100 ft/min).
2. Configurations:
   - Longitudinal full forward-CG: “constant fast” acceleration that gives the pitch attitude equal or higher to full forward CG (acceleration)

- Longitudinal full aft-CG: “constant fast” deceleration that gives the pitch attitude equal or higher to full aft CG (deceleration)
- Longitudinal slight forward CG: “constant slow” acceleration;
- Longitudinal slight aft CG: “constant slow” deceleration.

The calibrated airspeed and pressure altitude used as ground truth could be provided by a GPS calibration method or a calibrated system. Ideally, only GPS data recorded from a flight in the absence of wind, once corrected for air density, together with VS, should be used as the calibrated datum. In practice, in the case of wind, the HW-TW method could be applied to remove the effect of wind.
Using the HW-TW method, it was possible to demonstrate that the pitot-static sensors installed on the nose-boom could be calibrated in such a way that the residual airspeed errors are generally close to zero, and in the worst cases they reach +-2 kts at the extremes of flight conditions and rotorcraft configurations (see **Figure 26**).

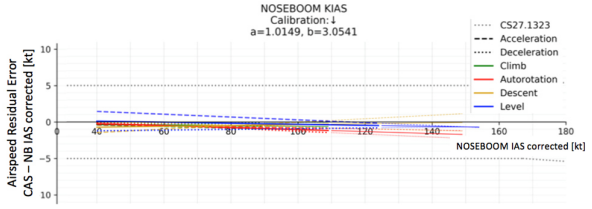

Figure 26- HW- TW, Nose-boom residual errors for all flight regimes

In fact, the AW09 P3 nose-boom installation remained affected by a relatively small position error (airspeed under-reading due to overpressure) and marginally affected by AOA and AOS. A Nose-boom installation further forward or moved on the side, might help further reduce the residual error.

It was decided to use the calibrated nose-boom data for the research. Therefore, the required data could come from flight tests not specifically dedicated to pitot-static calibration and it was not necessary to perform the vector calculation (GPS method). The data used to train the NNR came from two flights which covered a very broad flight envelope and aircraft configurations (accelerations and decelerations).
The helicopter configuration was set to mid-weight configuration and mid-CG longitudinal position. The automatic extraction of test points returned 3.600 test points, which have been used during the Learning phase and the Validation phase.

4.3 Neural Network Regressor selection

The most robust algorithm was proved to be a fully connected Neural Network Regressor (NNR) with two hidden layers which has a $relu$ transfer function on the first two layers and a $tanh$ function in the output layer. The structure of the algorithm can be represented as follows (see also **Figure 27**):

$$CAS = \tanh(C_3 \cdot \mathrm{relu}(C_2 \cdot \mathrm{relu}(C_1 \cdot X + I_1) + I_2) + I_3) \quad (27)$$

The flight test points were automatically selected from generic flights using search algorithms inspired by big-data and in particular map-reduce functions (to process huge amounts of flight data in a short time). An algorithm was used that identified 2-second test points and averaged the pitch angle, VS, uncorrected airspeed and uncorrected static pressure (all parameters taken from the production air data systems).

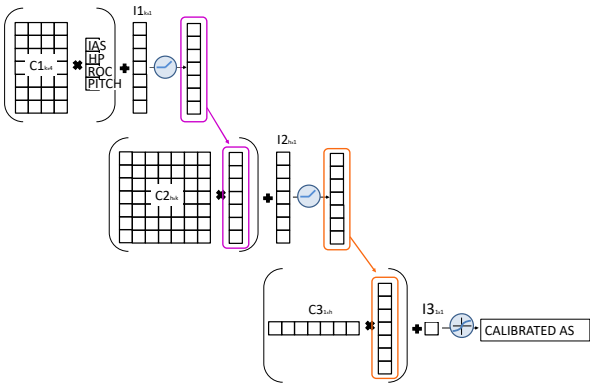

Figure 27–Neural Network Regressor structure example for pitot-static correction

The NNR calibration function represents a mapping extended to all the flight regimes and configurations of the production Air Data Sensor Error as a function of the input parameters.

4.4 Convergence of NNR weight adjustment

Each parameter has been normalized before the training and de-normalized (using the inverse normalization function) after the execution of the algorithm.
The dataset has been split into two groups, 90% of test points have been used for training the algorithm, the remaining 10% has been used to obtain the loss function and validate the convergence. The structure of the NNR is a fully connected feed-forward NNR. The weights of the functions have been approximated using a classic Back-Propagation algorithm and the solver used to estimate the gradient moment is *Adam*[5].
The number of Hidden Layers as well as the Number of Neurons per hidden layer and the transfer function used has been at the center of an extensive optimization analysis. The objectives of the optimization were:

- Minimize the number of weights to reduce the required memory of the NNR function when implemented in an embedded system.
- Perform a “good” fitting of the error data.
- Do not show warps of the calibration curves outside of the tested envelope.

The results are mostly based on expert judgment. Some qualitative considerations can be drawn based on the error curves obtained (see **Figure 29** and **Figure 30**):

- The neural network requires at least two hidden layers but more than 2 hidden layers are not necessary.
- The output layer transfer function must be always the hyperbolic tangent $tanh$.

- The accuracy of the estimation is not dependent on how the neurons are split between Hidden Layer 1 and Hidden Layer 2 but only on their overall number.
- The transfer function to use in the Hidden Layers is the $RELU$ function, as the calibration lines follow much more the data distribution. By using $tanh$ transfer functions in the Hidden Layers, the accuracy of calibration lines is significantly reduced.
- By using the $RELU$ transfer function, the accuracy of the algorithm becomes much more precise as the number of parameter increases. Instead, by using the $tanh$ function, the NN algorithm suffers from the gradient descent problem and the approximation becomes too linear.
- Despite the $RELU$ function allows to obtain a better calibration, the number of parameters required to have a "smooth" calibration curve is significantly high; A good compromise is to use 2 Hidden Layers with 300 neurons each or to use the $GELU$ transfer function.

The final result can be seen in **Figure 31**, where the optimal calibration has been chosen to represent the Airspeed error.

4.5 Implementation of Real-Time calibration

The research demonstrated that matrix calculation for the calibration of the Airspeed and Pressure Altitude data in real time, does not require extensive resources to be implemented to obtain errors which are minimal for all the flight conditions. This type of corrections could open the door to more safe flights and optimized aircraft designs. Preliminary results (see **Figure 32**) show that the calibration using a Neural Network (Process 3), in blue, could significantly reduce the airspeed and altitude errors even in those conditions where the state of art corrections still have high residual errors (Process 2). In red the un-calibrated datum (Process 1) is provided as a reference.
In particular, classic methods still present errors when the Vertical Speed is not close to zero, see the last subplot. Also in this case the correction provided using a Neural Network Regressor offers optimal performance and almost zero error in all flight regimes.

4.6 Off line calibration calculation

The research further explored the possibility to off-line calculate the calibration errors using relevant settings and parameters. For this it was required to develop an extended algorithm which also estimates the pitch attitude based on other parameters such as: Horizontal Stabilizer Geometrical Pitch (configuration of the helicopter), Longitudinal CG Position, Longitudinal Speed Rate (Long. Acceleration/Deceleration), Vertical Speed, uncorrected Airspeed and uncorrected Pressure Altitude. The general structure is described in **Figure 28**.

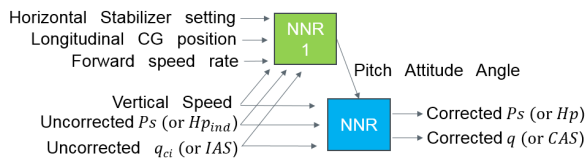

Figure 28– Possible extension of Neural Network Regressor also estimating the Pitch Angle

Using the NNR it is possible to provide a range of input parameters and estimate how the sensor performs in every condition in the Flight Envelope.
Figure 33 presents the estimate error in various points of the flight envelope, involving various pressure altitudes, various CG positions, various ROC and evaluated for IAS between 30kts and 160kts.
The qualitative check of the lines also allows to state that during the training phase, the algorithm was not subject to over-fitting the data points. In particular, the algorithm developed has been proven to be robust in presence of noise in the data. It should be noted that the data set required for the first regressor in **Figure 28** did not require the installation of the final configuration of the production pitot-static systems and could come from a wider range of flight tests not necessarily dedicated to pitot-static calibration.

4.7 Comments on test execution & data processing

Of paramount importance has been the selection of sensors which could indicate accurate and precise data, both in space and in time. As an example the nose-boom, which has been selected as reference datum to calibrate the NNR, presents a very small error in all flight conditions which has been corrected.
Also the GS and $Pitch$ sensor selection must ensure a very accurate position estimation; Usually the implementation of a Kalman Filter guarantees the required standards of precision and accuracy.

5. CONCLUSIONS

The proposed numerical methods could be used to generate calibration curves for state-of-the-art Air Data Units in order to calculate and optimize residual airspeed and altitude errors for all combinations of flight regimes and aircraft configurations. The required calibration data can be collected with modern quasi-static GPS methods that provide results practically identical to classical methods with a reduced amount of flight test activities and reduced costs.
The calibration used by the state-of-the-art Air Data Unit, which is based on static and dynamic pressure errors associated only with the measured dynamic pressure, does not guarantee that residual errors and out-of-bounds differences between production pitot-static systems are always acceptable. This leads to a high design effort and the risk of redesigning and re-testing pitot-static systems.
The proposed new methodology, based on a multi-input regressor using a fully connected neural network, is able to provide real-time indications of the correct speed and altitude for any combination of flight conditions and aircraft configuration. In this way, on one hand the aircraft manufacturer will be able to optimize development and production costs and increase ground safety, on the other the correct value of speed and altitude data will be always guaranteed in flight.

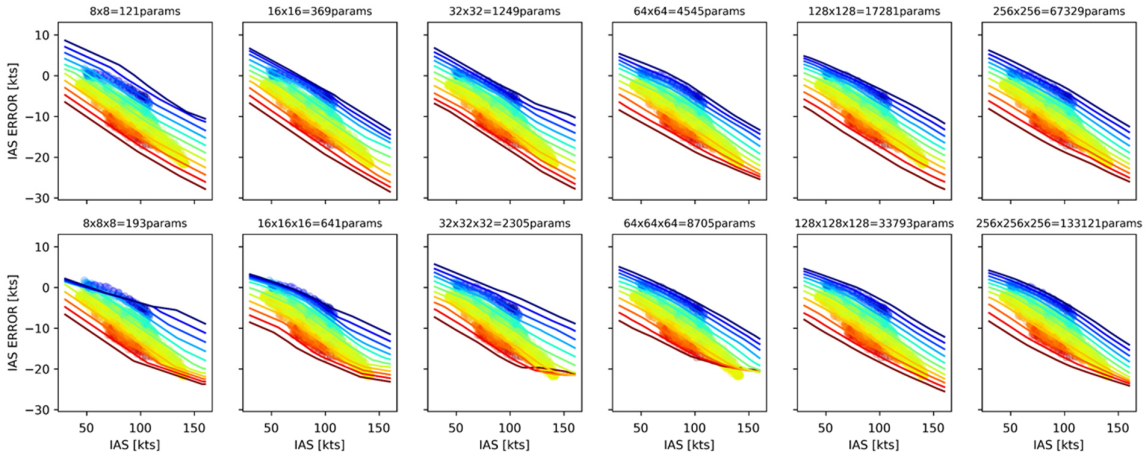

Figure 29– ADAHRS Error, Flight Test data approximation by various NN structures using RELU on hidden layers.

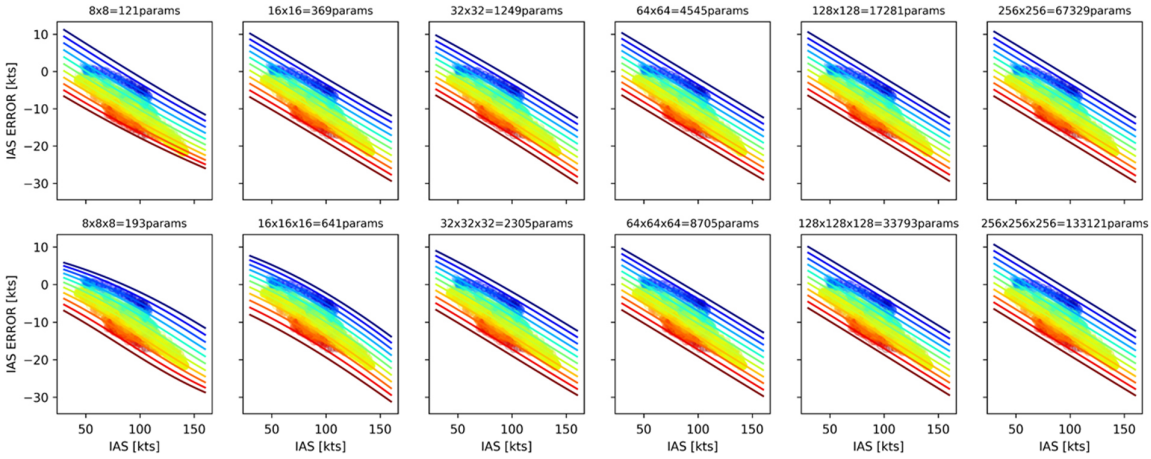

Figure 30– ADAHRS Error, Flight Test data approximation by various NN structures using TANH on hidden layers.

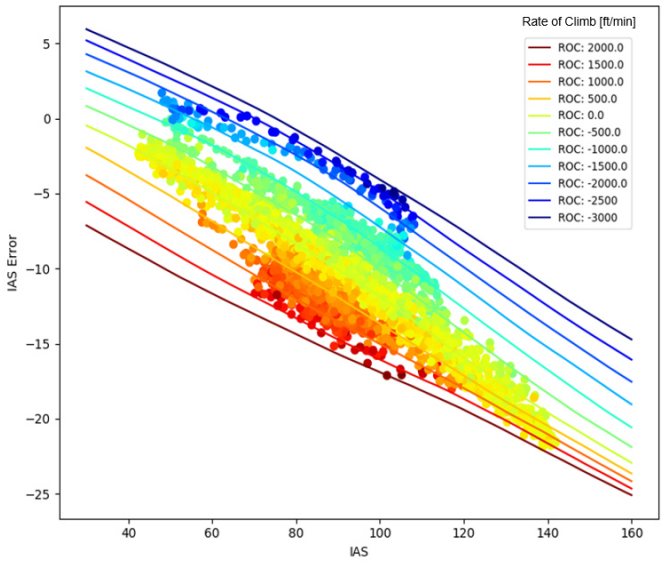

Figure 31– ADAHRS airspeed error, Flight Test data approximation by final NNR structure.

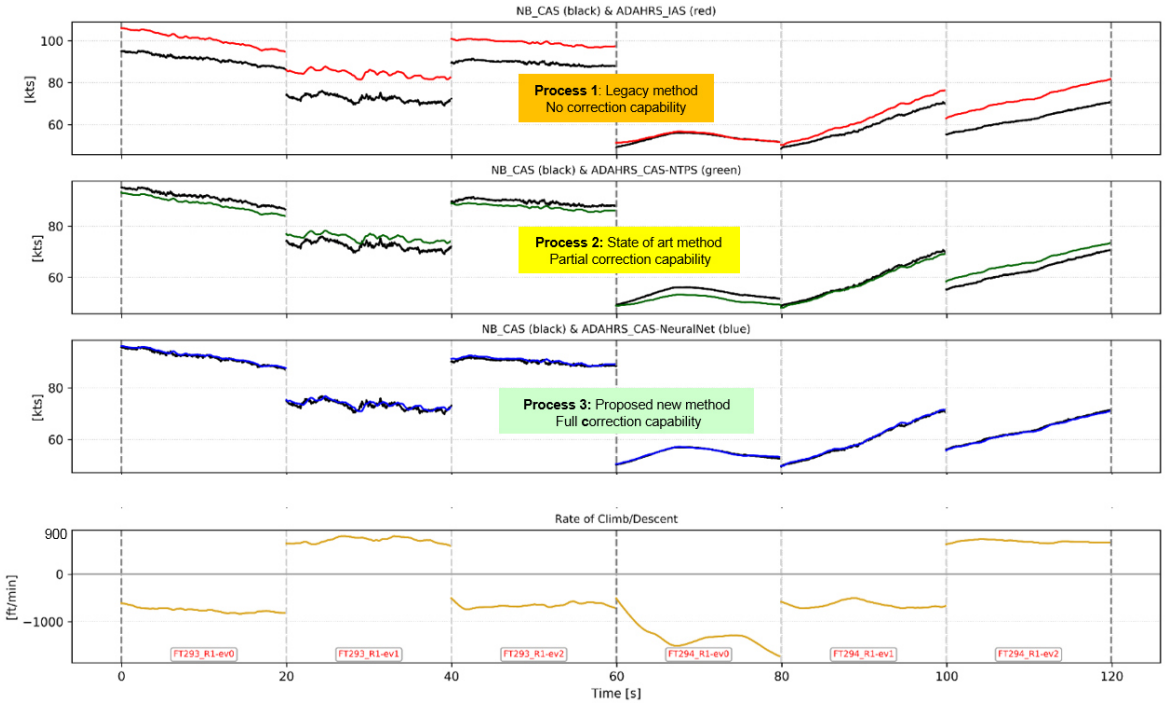

Figure 32– Airspeed calibration in real time: Neural Network calibration provides less error compared to traditional calibrations

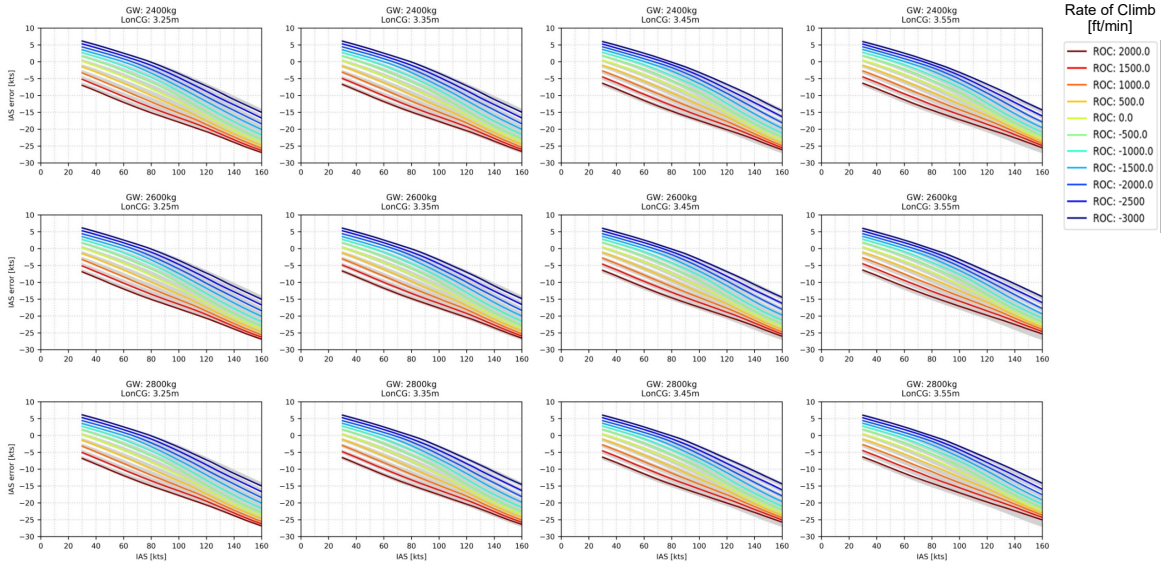

Figure 33– Airspeed calibration curves – Acceleration -1 kt/sec – 5000 ft Hp.

6. REFERENCES

1. *Gray, Doug. "Using GPS to accurately establish True Airspeed (TAS)." National Test Pilot School, June (1998).*
2. *Hamel, Kolarich. "GPS-based Airspeed Calibration for Rotorcraft (Generalized Application for All Flight Regimes) method". Presented at the Vertical Flight Society's 76th Annual Forum & Technology Display, Oct (2020)*
3. *Rao, C. Radhakrishna, and Sujit Kumar Mitra. "Generalized inverse of matrices and its applications John Wiley & Sons." Inc., New York-London-Sydney (1971).*
4. *Jolliffe, I. T. "Principal Component Analysis. Springer Series in Statistics". Springer-Verlag. pp. 487. ISBN 978-0-387-95442-4. (1986)*
5. *Kingma, Diederik P., and Jimmy Ba. "Adam: A method for stochastic optimization." arXiv preprint arXiv:1412.6980 (2014).*